Geophysical Research Letters

RESEARCH LETTER
10.1029/2020GL092130

Nikita Kaushal and Nivedita Sanwlani contributed equally to the work.

Key Points:

- We show that luminescence in coral skeletons is a proxy for terrestrial chromophoric dissolved organic matter (CDOM)
- This proxy yields information on land-to-ocean dissolved organic matter (DOM) flux in historically under-sampled tropical seas
- A 24-year reconstructed CDOM record from Borneo shows large seasonal DOM flux from peatland, and likely influences of photodegradation

Supporting Information:

Supporting Information may be found in the online version of this article.

Correspondence to:

N. Kaushal, N. Sanwlani, and P. Martin,
nkaushal@ntu.edu.sg;
nsanwlani@ntu.edu.sg;
pmartin@ntu.edu.sg

Citation:

Kaushal, N., Sanwlani, N., Tanzil, J. T. I., Cherukuru, N., Sahar, S., Müller, M., et al. (2021). Coral skeletal luminescence records changes in terrestrial chromophoric dissolved organic matter in tropical coastal waters. *Geophysical Research Letters*, *48*, e2020GL092130. https://doi.org/10.1029/2020GL092130

Received 15 DEC 2020
Accepted 24 MAR 2021

Coral Skeletal Luminescence Records Changes in Terrestrial Chromophoric Dissolved Organic Matter in Tropical Coastal Waters

Nikita Kaushal[1], Nivedita Sanwlani[1], Jani T. I. Tanzil[3,4], Nagur Cherukuru[5], Syamil Sahar[6], Moritz Müller[7], Aazani Mujahid[6], Jen N. Lee[8], Nathalie F. Goodkin[1,2,9], and Patrick Martin[1]

[1]Asian School of the Environment, Nanyang Technological University, Singapore, Singapore, [2]Earth Observatory of Singapore, Nanyang Technological University, Singapore, Singapore, [3]St. John's Island National Marine Laboratory, National University of Singapore, Singapore, Singapore, [4]Tropical Marine Science Institute, National University of Singapore, Singapore, Singapore, [5]CSIRO Oceans and Atmosphere, Canberra, ACT, Australia, [6]Faculty of Resource Science & Technology, University Malaysia Sarawak, Kota Samarahan, Malaysia, [7]Faculty of Engineering, Computing, and Science, Swinburne University of Technology Sarawak Campus, Kuching, Malaysia, [8]Faculty of Science and Marine Environment, Universiti Malaysia Terengganu, Terengganu, Malaysia, [9]Department of Earth and Planetary Sciences, American Museum of Natural History, New York, NY, USA

Abstract

Terrigenous dissolved organic matter (tDOM) carried by rivers represents an important carbon flux to the coastal ocean, which is thought to be increasing globally. Because tDOM is rich in light-absorbent chromophoric dissolved organic matter (CDOM), it may also reduce the amount of sunlight available in coastal ecosystems. Despite its biogeochemical and ecological significance, there are few long-term records of tDOM, hindering our understanding of its drivers and dynamics. Corals incorporate terrestrial humic acids, an important constituent of CDOM, resulting in luminescent bands that have been previously linked to rainfall and run-off. We show that luminescence green-to-blue (G/B) ratios in a coral core growing in waters affected by peatland run-off correlate strongly with remote sensing-derived CDOM absorption. The 24-year monthly resolution reconstructed record shows that rainfall controls land-to-ocean tDOM flux from this protected peatland catchment, and suggests an additional impact by solar radiation, which degrades tDOM at sea.

Plain Language Summary

A critical priority in biogeochemistry is to improve our understanding of the global carbon cycle so that we can make accurate predictions of future CO_2 concentrations. One important but still enigmatic aspect of the carbon cycle is the transport and fate of organic carbon from soils to the ocean. Our understanding of this flux is particularly limited by the lack of historical time-series measurements. One way of obtaining such historical data is through satellite-derived measurements, but this can only yield data for the most recent decades. Here, we show that historical records of terrestrial carbon can also be reconstructed from luminescence measurements of coral cores, which have the potential to yield centuries-long time series of carbon concentrations. Corals are carbonate archives that record different environmental parameters during their skeleton formation. Luminescence is caused by the incorporation of humic acids, an integral component of terrestrially derived dissolved organic carbon. Our 24-year long reconstruction from a coral core collected off Borneo suggests that organic carbon concentrations are driven by rainfall over adjacent peatlands, and by solar radiation that breaks down the organic carbon at sea. There is no long-term shift, suggesting that this peatland catchment has stayed protected from land-use change.

1. Introduction

The flux of terrigenous dissolved organic carbon (tDOC) from land to sea is quantitatively significant in the global carbon cycle, but the fate of tDOC in the ocean remains poorly known (Ciais et al., 2014; Cole et al., 2007). In some regions, a potentially large fraction of this tDOC flux can be oxidized to CO_2 through photodegradation and biodegradation processes, contributing to coastal ocean acidification and ultimately degassing to the atmosphere (Fichot et al., 2014; Semiletov et al., 2016; Ward et al., 2017). Moreover, tDOC is rich in chromophoric dissolved organic matter (CDOM), which is the fraction of dissolved organic matter

that absorbs light. CDOM plays an important role in aquatic ecosystems by absorbing sunlight and reducing its transmission through the water column (Kowalczuk et al., 2005; Mascarenhas et al., 2017). This is partly beneficial for aquatic life: photodegradation can release nutrients from refractory organic compounds (Bushaw et al., 1996), while absorption of ultraviolet radiation protects biota (Dunne & Brown, 1996; Pienitz & Vincent, 2000). However, light absorption by CDOM also reduces the availability of light for primary producers, which particularly affects benthic ecosystems such as seagrass meadows, kelp forests, and coral reefs (Gattuso et al., 2006; Jones, 1998).

Long-running measurements have shown that tDOC fluxes in North America and Europe have increased in recent decades. While this is largely attributed to reductions in atmospheric pollution, changes in climate and land-use have also contributed to these increases (Evans et al., 2005; Monteith et al., 2007; Noacco et al., 2017; Wauthy et al., 2018). Land-use change, in particular, is thought to have accelerated land-ocean organic carbon fluxes world-wide (Butman et al., 2015), and may have led to particularly dramatic increases in tDOC fluxes from disturbed peatlands in Southeast Asia (Moore et al., 2013; Yupi et al., 2016). Given the ecological and biogeochemical impacts of tDOC on coastal ecosystems, the implications of such increases in tDOC fluxes are potentially profound. Indeed, indirect evidence from parts of northern Europe suggests that increases in terrestrial CDOM have reduced light availability sufficiently to have noticeable ecological impacts (Aksnes et al., 2009; Frigstad et al., 2013). However, even in the best-studied parts of the world (i.e., Europe and North America) we still largely lack long time-series of tDOC dynamics in coastal waters. Across the tropics, there are no such observational time-series data, even though tropical rivers contribute around half of the global land-ocean tDOC flux (Dai et al., 2012).

Currently, this paucity of time series can only be overcome using optical remote sensing, which allows CDOM to be calculated from the water-leaving reflectance spectrum (Odermatt et al., 2012). This offers high spatial and temporal coverage, and in many coastal locations, CDOM or the CDOM spectral characteristics can then be used to infer DOC or even tDOC concentrations (Fichot & Benner, 2012; Liu et al., 2019; Shanmugam, 2011). However, to measure tDOC from satellite remote sensing in optically complex coastal waters still requires regional algorithms to be developed, which first necessitates a substantial effort to collect optical and biogeochemical data in the field. Consequently, such remote sensing analyses only exist for a limited number of locations (ChunHock et al., 2020; D'Sa et al., 2006; Mannino et al., 2008; Siswanto et al., 2011). Moreover, remote sensing can only extend records of coastal CDOM back over the past few decades, and cannot measure through cloud cover or during the dark, which limits the utility of this technique, especially in equatorial and polar regions. It is therefore highly attractive to look to possible natural archives for longer-term time series of CDOM and tDOC.

Humic-like substances are an integral component of tDOC, and an important constituent of the CDOM pool (Coble, 2007). The term encompasses a mixture of high-molecular-weight substances formed during the partial decomposition of terrestrial organic matter in soils (Piccolo et al., 2018). They are strongly fluorescent (Coble, 2007), and corals incorporate such humic-like substances into their skeletons during growth, where they can form sub-annual growth layers that luminesce under ultraviolet (UV) light (Matthews et al., 1996; Susic et al., 1991; Tanzil et al., 2016). Such molecules most likely diffuse passively to the coral calcification site *via* paracellular pathways through the coral tissue (Tambutté et al., 2012). Corals such as *Porites* spp. also offer exceptional chronological constraints, allowing monthly resolution proxy reconstructions over hundreds of years. Coral core luminescence has been used to reconstruct past rainfall and river discharge from the Burdekin River on the Great Barrier Reef (Isdale, 1984; Isdale et al., 1998; Lough, 2007; Lough et al., 2002; Rodriguez-Ramirez et al., 2014), in Madagascar (Grove et al., 2012, 2013; Maina et al., 2012) and correlates with salinity in Southeast Asia (Tanzil et al., 2016).

Using fluorescence excitation-emission matrix measurements, we recently demonstrated that coral luminescence is quantitatively related to the fluorescence intensity of terrestrial humic substances and that terrestrial humic substances, but not plankton-derived marine humic substances, are preferentially incorporated into aragonite (Kaushal et al., 2020). Because humic substances are such a key component of terrestrial CDOM and therefore of tDOC, this implies that coral luminescence is more directly a proxy for terrestrial CDOM and tDOC. Coral luminescence is more indirectly a proxy for rainfall or salinity to the extent that terrestrial CDOM and tDOC are typically closely related to salinity in shelf seas (Carr et al., 2019; Fichot et al., 2014; Martin et al., 2018). Here, we show that coral skeletal luminescence is indeed an accurate

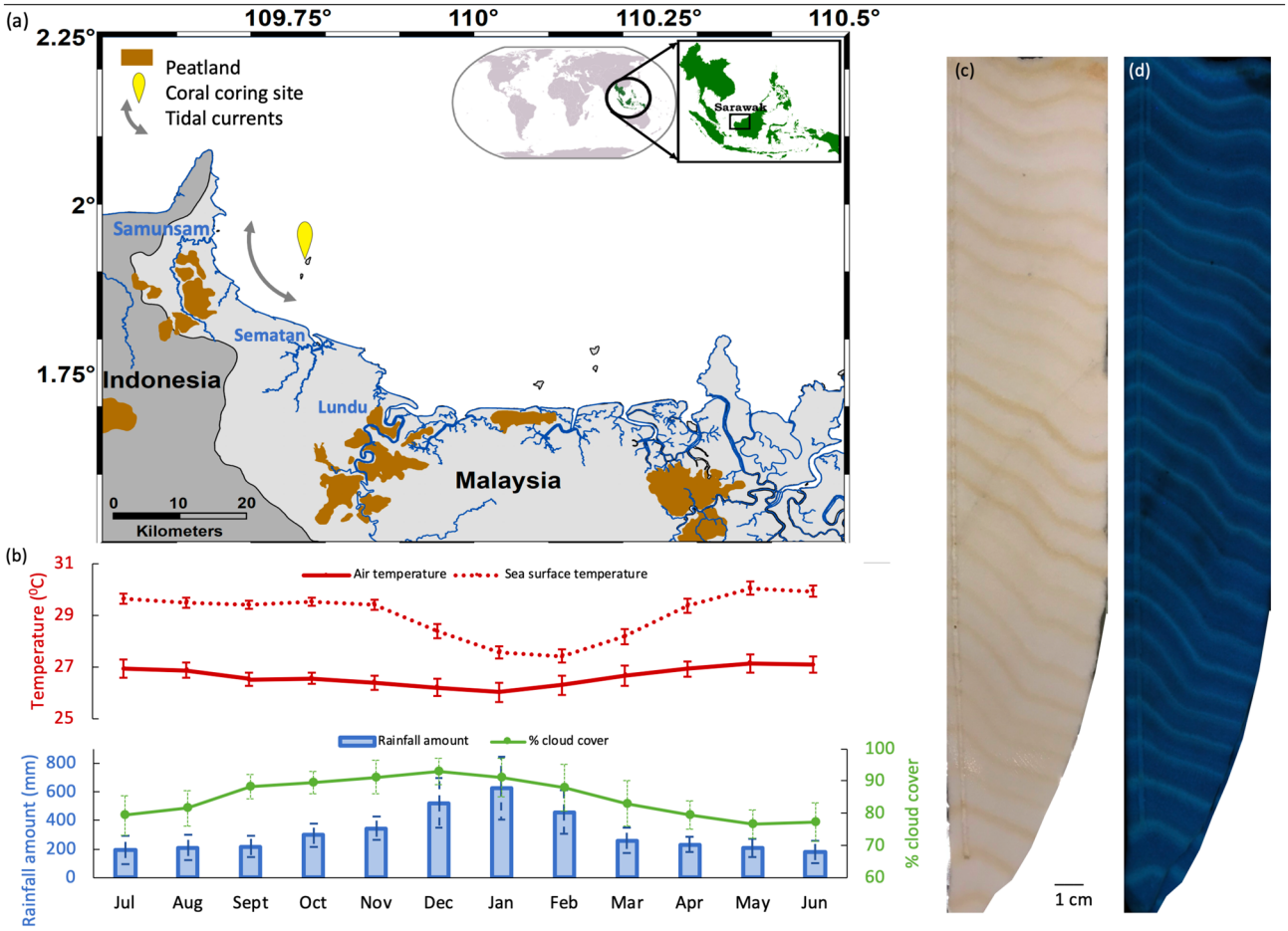

Figure 1. (a) Coral collection site in Sarawak, Malaysia, showing the main river systems and peatland cover (the latter from Global Forest Watch and Dommain et al., 2014). (b) Monthly mean and standard deviation for temperature, rainfall, and percentage cloud cover for 1990–2014. Data sources: monthly mean air temperature: CRU TS4.04 109.5°–110.5°E and 1.5°–2.5°N (Jones & Harris, 2008); monthly mean sea surface temperature: HadISST 1.1 109.0°–111.0°E and 1.0°–3.0°N (Rayner et al., 2003); rainfall amount: GPCC 109.5°–110°E and 1.5°–2.0°N; percentage cloud cover: CLARA-A2 109.5°–110°E and 1.75°–2.25°N (Karlsson et al., 2017). Data obtained from KNMI Explorer. (c) Talang coral core in true color and (d) luminescence image under UV excitation.

proxy for terrestrial CDOM, by calibrating coral core luminescence with a 12-year time series of satellite-derived CDOM from north-western Borneo. We then reconstruct a 24-year record of terrestrial CDOM with this core and investigate monthly- to annual-scale drivers of tDOM variability in this region.

2. Materials and Methods

2.1. Study Site

The coral core was collected from the western coast of Pulau Talang Besar (1.918°N, 109.774°E), which is part of a National Park referred to here as the Talang Islands. These small islands are situated in the southern South China Sea, 20 km off the western coast of Sarawak, Malaysian Borneo (Figure 1a). Martin et al. (2018) and Zhou et al. (2019) reported characteristics of chromophoric and fluorescent DOM of rivers and coastal waters in this region. The Talang Islands are chiefly affected by the Samunsam River, which is a peatland-draining blackwater river that carries very high concentrations of DOC (1,200–1,800 μmol L^{-1}) and CDOM (reported as absorption coefficient at 350 nm, $a_{CDOM}(350)$, of 71–98 m^{-1}). The Sematan and Lundu rivers drain catchments with limited peatland cover and carry much less DOC (240–500 μmol L^{-1}) and CDOM ($a_{CDOM}(350)$: <15 m^{-1}). Despite seasonal changes in the DOC and CDOM concentrations, the relationship between DOC and CDOM across all the coastal waters and rivers sampled was very strong and showed no seasonality, demonstrating that CDOM is an effective proxy for tDOC in this region (Martin

et al., 2018). Furthermore, Zhou et al. (2019) estimated from fluorescent DOM distributions that at least 20%–40% of the total DOC in coastal waters was terrigenous DOC.

Sarawak has an equatorial climate with rainfall throughout the year, but rainfall approximately doubles during the Northeast Monsoon (December–February) relative to other months (Figure 1b). The cloud cover exceeds 70% year-round but is lower during April to August. Sea surface temperature (SST) decreases around 2°C from December to March, but the air temperature is close to 27 °C in all months, dropping by only 0.5°C during the Northeast Monsoon.

2.2. Coral Collection, Age Model, and Luminescence Measurements

The coral core was collected in May 2015 from the main growth axis of a *Porites* sp. colony at 2–3 m depth using a pneumatic drill with a 5-cm diameter, 50-cm length diamond bit core barrel. A slice of ∼0.7 cm was cut and cleaned for 48 h with a 1:4 mix of household bleach (NaOCl, 3%–7% reactive chlorine), and sonicated in deionized water for 30 min (water changed every 10 min). Bleaching removes contaminants and increases the luminescence intensity (Nagtegaal et al., 2012). The cleaned section was photographed under UV light (excitation wavelength 365 nm) using spectral line scanning (SLS) on an Avaatech XRF scanner (Grove et al., 2010, 2015; Tanzil et al., 2016). The light source and camera are moved down the core as one unit scanning multiple lines that are stitched together to produce a continuous image. The light entering the camera lens is split into three wavelength bands (red, green, blue) by a dichroic RGB beam splitter prism and is recorded by separate sensors. The luminescence green-to-blue ratio (G/B ratio) for the coral section was obtained along the main growth axis for a 2-mm wide track at a resolution of 143 pixels cm^{-1}. The G/B ratio was shown to be a more accurate tracer of terrestrial input than total luminescence, because the ratio normalizes for luminescence variation caused by other factors, such as variation in skeletal microstructure (Grove et al., 2010). The age model was constructed by considering each peak luminescence G/B layer as the Northeast Monsoon peak of each year with the upper-most layer as the Northeast Monsoon of 2014. We assumed that the coral had a linear growth rate between adjacent peaks, amounting to a growth rate of ∼1 cm/year. These assumptions are reliable in numerous *Porites* sp. cores collected across Southeast Asia (Tanzil et al., 2016, 2019). For this study, a core section of ∼25 cm in length covering 24 years of growth from 1990 to 2014 was selected.

2.3. Satellite-Derived CDOM Measurements

We used the MODIS-Aqua Collection 6.1 Level 2 ocean color product, with 1-km resolution, from https://oceancolor.gsfc.nasa.gov/for the period July 2002 to June 2014. MODIS was selected because of its high (daily) revisit frequency. The MODIS data were processed with a regionally parameterized inversion model, described in Cherukuru et al. (2021), based on the Generalized Inherent Optical Property model (Werdell et al., 2013). Briefly, this model uses a spectral optical library of in situ biogeochemical and optical measurements and estimates the concentrations of CDOM, DOC, and total suspended matter (TSM) based on selecting the most suitable set of specific inherent optical properties (SIOPs) from the optical library. This selection is made for each pixel in the satellite image by identifying which of the in situ measured remote sensing reflectance spectra in the optical library best matches the MODIS-measured remote sensing reflectance and then selecting the SIOPs of the stations where the matching reflectance spectrum was measured. The SIOPs are the DOC-specific CDOM absorption (i.e., absorption per unit DOC), the TSM-specific particulate absorption, and the TSM-specific backscattering. These SIOPs are then used in a forward model to simulate the best match between forward-modeled remote sensing reflectance and MODIS-measured remote sensing reflectance by iteratively varying the DOC and TSM concentrations and deriving the inherent optical properties according to the SIOP values.

We used the model to retrieve a time series of CDOM, quantified as the CDOM absorption coefficient at 440 nm, $a_{CDOM}(440)$. This represents the absorption of light at 440 nm by CDOM over a unit of distance, and is reported in units of m^{-1}. To create a satellite-derived time series of CDOM absorption to compare to the coral core data, we calculated the average $a_{CDOM}(440)$ at daily resolution over a 3 × 3 km area immediately west of the Talang Islands, centered at 1.914°N 109.741°E, and further calculated the monthly averages of satellite-derived CDOM.

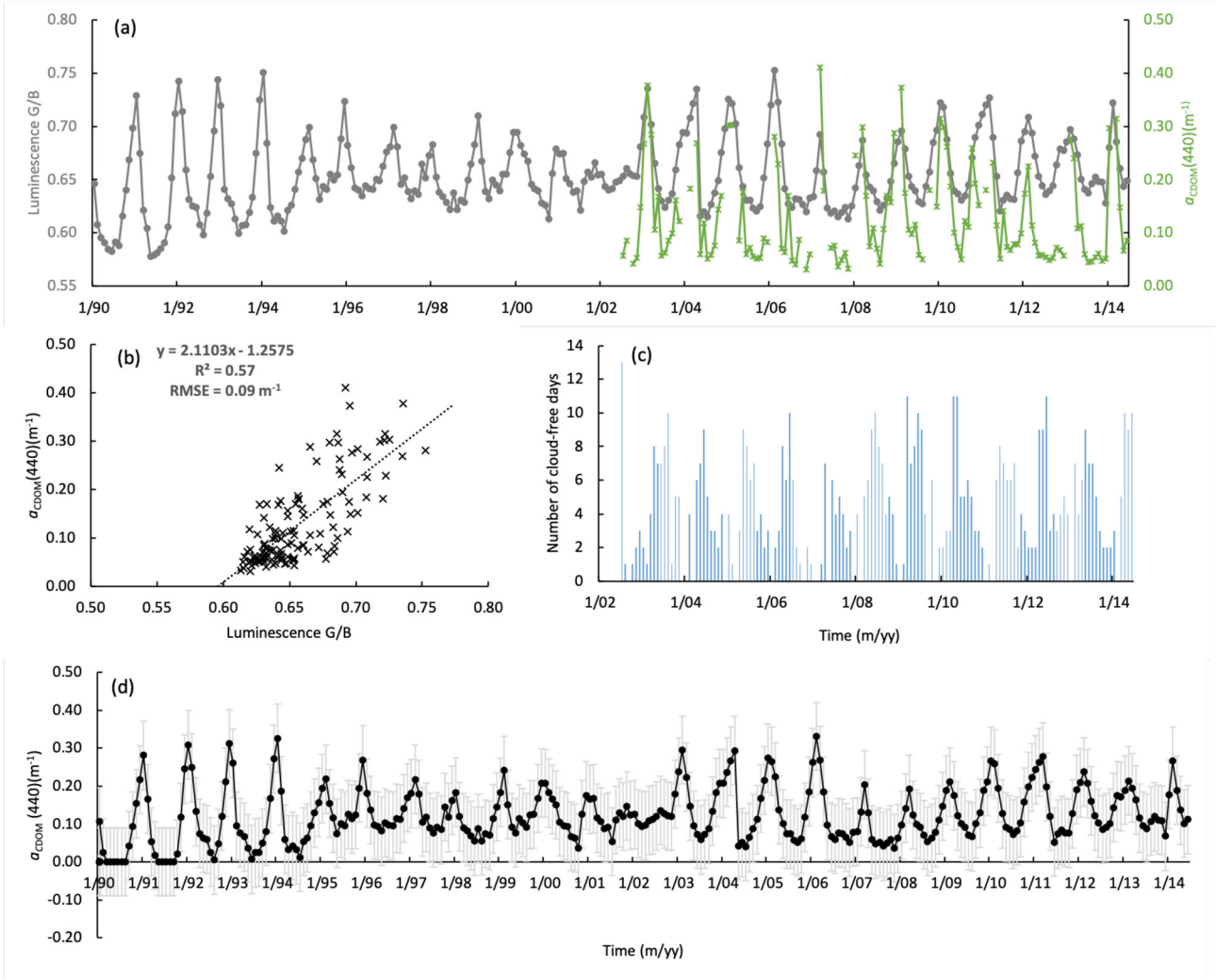

Figure 2. (a) Luminescence green-to-blue (G/B) ratios of the Talang coral core and satellite-derived $a_{CDOM}(440)$ showed strong seasonal variation with a clear peak during the Northeast Monsoon. The breaks in the $a_{CDOM}(440)$ indicate months with missing data. (b) Luminescence G/B showed a strong linear relationship against satellite-derived $a_{CDOM}(440)$ ($R^2 = 0.57$, RMSE = 0.09 m^{-1}). (c) The number of cloud-free days in the satellite record. (d) Reconstructed $a_{CDOM}(440)$ time series. Error bars represent RMSE of ±0.09 m^{-1}.

2.4. Peak Alignment

The time series of coral core G/B ratio and of monthly mean $a_{CDOM}(440)$ both showed well-defined seasonal peaks during the late Northeast Monsoon, with $a_{CDOM}(440)$ typically peaking in February. We peak-aligned the time series of coral G/B ratio with satellite-derived $a_{CDOM}(440)$ maxima and minima using Analyseries 2.0 (Paillard et al., 1996). This process rescales the luminescence G/B data and gives monthly averaged luminescence G/B.

3. Results

3.1. Proxy Development

The Talang coral luminescence green-to-blue ratio (G/B ratio) ranged between 0.58 and 0.75 from January 1990 to June 2014 (Figure 2a). Twenty-two of the 24 years of monthly measurements show a single distinct luminescence peak every year with the notable exceptions of 2001 and 2002, where multiple months show values around 0.65 without the single distinct peak >0.68 seen in other years.

The satellite-derived CDOM absorption, $a_{CDOM}(440)$, ranged between 0.03 and 0.41 m^{-1}, with a single peak observed each year (Figure 2a). The peak was usually in February, that is, during the late Northeast Monsoon, with a few years showing a peak in the later months of March and April. Owing to cloud cover, the Northeast Monsoon months of December to February have the fewest measurements, with some months having only a single day of data. The months of April to August have the lowest cloud cover and therefore highest data counts of >3 days a month (Figure 2c). For 17 of the total 143 months, there are no cloud-free data.

The time series of satellite-derived $a_{CDOM}(440)$ and coral G/B ratio showed highly correlated seasonality (Figure 2a). We calibrated the G/B ratio as a proxy for $a_{CDOM}(440)$ using the full monthly resolution time series from July 2002 to June 2014. This revealed a strong linear relationship:

$$a_{CDOM}\left(440\right) = 2.1103 \times \text{Luminescence G/B} - 1.2575,$$

with $R^2 = 0.57$ and RMSE of 0.09 m^{-1} (Figure 2b). We then applied this relationship to reconstruct CDOM from the G/B ratio through the full length of the coral core (1990–2014), providing a ~24-year record of CDOM.

The reconstructed $a_{CDOM}(440)$ record ranged between 0 and 0.35 m^{-1}, with a single peak each year (Figure 2d). Two short sections in 1990 (March–August) and 1991 (May–September) had G/B ratios <0.6, yielding slightly negative reconstructed $a_{CDOM}(440)$ values that were set to 0. There was strong seasonality, with $a_{CDOM}(440)$ peaking between December to March, likely driven by seasonal changes in climatic drivers. There is a small step-change in the record for the $a_{CDOM}(440)$ minima during the Southwest Monsoon, with very low values (<0.01 m^{-1}) before 1995 giving way to higher minima thereafter (>0.03 m^{-1}). Despite this increase in the Southwest Monsoon minima, there was only a small and statistically nonsignificant long-term trend in the annually averaged $a_{CDOM}(440)$ (linear regression, 0.0015 m^{-1} y^{-1}, $p = 0.19$). The Northeast Monsoon $a_{CDOM}(440)$ maxima do not show any systematic increasing trend, but there is a gradual shift in the timing of the $a_{CDOM}(440)$ peak, from January in the early 1990s to February after 2002. Overall, the time series shows large interannual variability in maximum and minimum $a_{CDOM}(440)$.

3.2. Seasonal and Interannual Drivers of CDOM Variability

The Northeast Monsoon peaks in $a_{CDOM}(440)$ are the most distinctive feature of the CDOM record (Figure 2d). Since this is the rainiest season, rainfall is the most obvious driver of the seasonal variation in CDOM. The month-to-month correlation (Spearman's rho) between reconstructed $a_{CDOM}(440)$ and monthly rainfall is 0.51 (Figure 3a), which increases to 0.53 if $a_{CDOM}(440)$ is lagged by one month (both $p < 0.05$). When the data are seasonally averaged, with the high-rainfall Northeast Monsoon months of December to February considered as one season and the remaining months as a second season, the correlation considerably increases to 0.68, since the seasonal averaging accounts for possible offsets between rainfall and $a_{CDOM}(440)$ accumulation at sea. Interestingly, we also found a month-to-month correlation between reconstructed $a_{CDOM}(440)$ and percentage cloud cover of lower, but still significant ($p < 0.05$) value of 0.40 (Figure 3b). When these data were seasonally averaged, with the low cloud cover months of April to August as one season and the remaining months as a second season, the correlation was 0.68, as high as the correlation of CDOM with seasonal rainfall. A surprisingly high correlation was also found between monthly $a_{CDOM}(440)$ and monthly SST, with $r_s = -0.59$ ($p < 0.05$), with lower SSTs corresponding to higher $a_{CDOM}(440)$ (Figure 3c). This correlation also increased when we averaged the data seasonally ($r_s = -0.64$) with the low SST months of December to March as one season and the remaining months as a second season. However, neither rainfall, cloud cover, nor SST were significantly correlated with $a_{CDOM}(440)$ when examined at annual resolution (all $p > 0.05$), indicating that none of these variables explained interannual variability in CDOM well. This is perhaps not surprising, since $a_{CDOM}(440)$ only varied between 0.07 to 0.15 m^{-1} interannually.

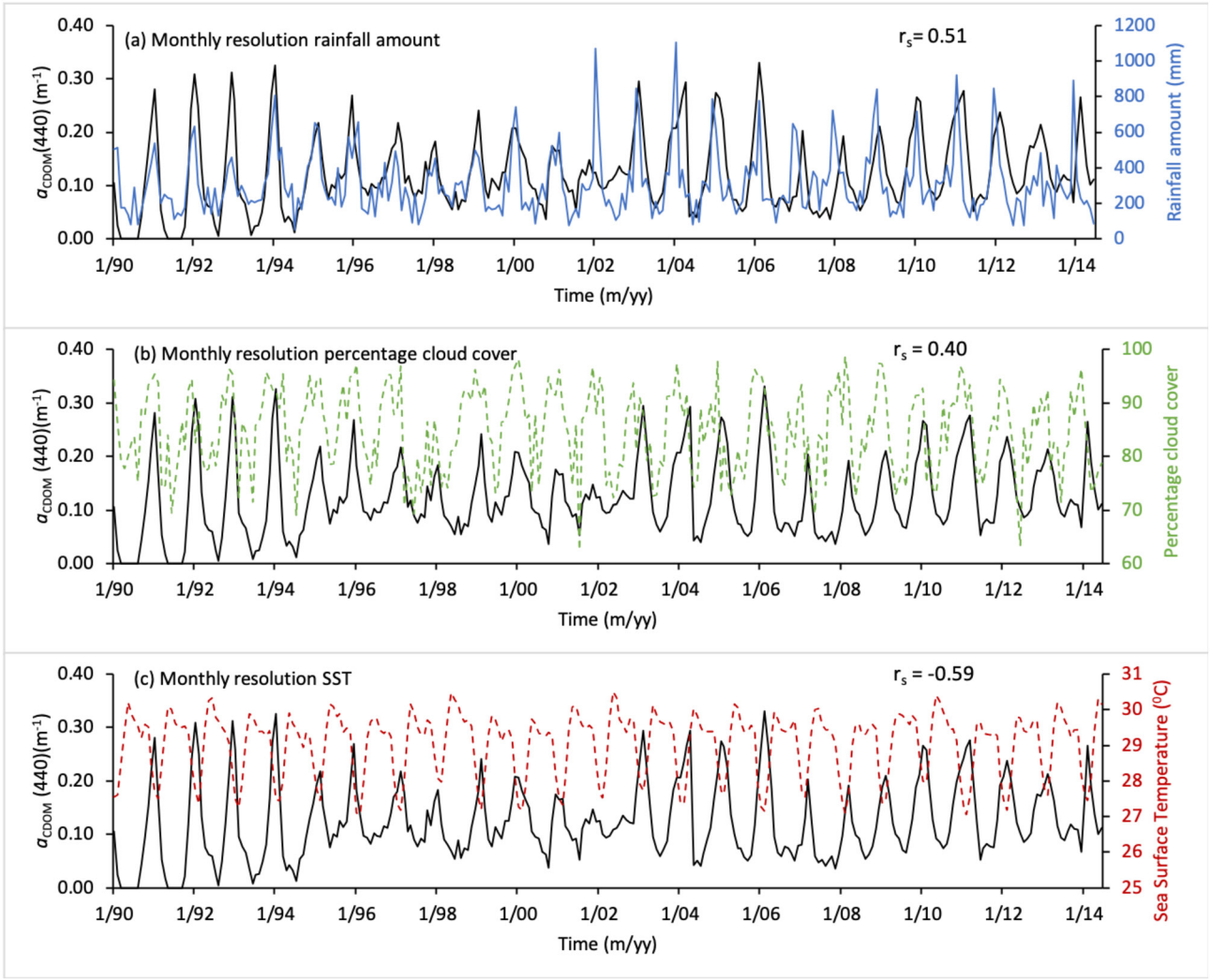

Figure 3. $a_{CDOM}(440)$ data plotted with monthly resolution (a) rainfall, (b) percentage cloud cover, and (c) SST. SST, sea surface temperature.

4. Discussion

Our results show that luminescence green-to-blue (G/B) ratios in coral cores are fundamentally driven by the concentration of terrigenous dissolved organic matter in the sea and that the variation in these ratios provides a palaeo-proxy for CDOM. The data gaps caused by cloud cover in our satellite record necessarily introduce uncertainties in our monthly mean CDOM estimates. Moreover, our satellite CDOM time series only represents snapshots at one time of day, which might be affected by short-term (e.g., tidal) variability that would be smoothed out in the coral record. These factors likely account for a large part of the scatter in our G/B versus CDOM relationship, and we anticipate that with better CDOM records, the calibration could prove to be considerably stronger. Nevertheless, the small RMSE of our calibration demonstrates that accurate CDOM reconstructions are possible.

This proxy is likely to reconstruct total CDOM accurately wherever the CDOM pool is dominated by terrestrially derived CDOM, such as in coastal waters of Southeast Asia that are influenced by peatland-draining rivers. Elsewhere, marine plankton is also a source of humic substances (Helms et al., 2013; Osburn et al., 2019). Such autochthonous marine CDOM usually differs spectrally from terrestrial CDOM (Astoreca et al., 2009; Painter et al., 2018; Stedmon & Markager, 2001). Although it has been speculated that such marine humic substances might also contribute to coral luminescent banding (Tudhope et al., 1996), aragonite precipitation experiments have shown that terrestrial humic substances are incorporated far more readily

compared to marine CDOM, yielding much higher fluorescence in the aragonite (Kaushal et al., 2020). This is consistent with previous studies showing that coral luminescent bands are a proxy for river discharge and salinity (Isdale, 1984; Isdale et al., 1998; Lough, 2007; Lough et al., 2002; Tanzil et al., 2016). However, if coral luminescence is in fact most directly a proxy for terrestrial CDOM, it becomes important to consider not only variation in CDOM input but also potential variation in CDOM removal, when interpreting luminescence records.

Our site is primarily exposed to discharge from the peatland-draining, DOC- and CDOM-rich Samunsam River (Figure 1). Seasonal changes in CDOM production in tropical peatlands are unlikely because of the small temperature range, and porewater concentrations of DOC, specific UV absorbance, and fluorescence of DOM appear to vary by ≤10% throughout the year (Gandois et al., 2013). The strong seasonal peak in CDOM during the Northeast Monsoon thus more likely points toward a rainfall-driven increase in land-to-sea CDOM flux, yet the monthly level correlation between reconstructed CDOM and rainfall was relatively weak. This may partly be due to an expected lag between rainfall on land and accumulation of CDOM at sea, yet a lagged correlation was only slightly stronger. While fluvial fluxes of DOC (and hence of CDOM) do generally increase with freshwater discharge both in peat and nonpeat soils (Clark et al., 2007; Moore & Jackson, 1989) the complex hydrology of peatlands means that DOC concentrations in peatland-draining rivers typically decrease during periods of high rainfall due to acrotelm overflow (Clark et al., 2007, 2008). This rainfall-driven dilution also occurs in Southeast Asian peatlands (Rixen et al., 2016), and is likely a reason for the higher DOC and CDOM concentrations measured in the Samunsam River in September compared to March (Martin et al., 2018). Consequently, the relationship between rainfall and the flux of DOC and CDOM to the sea is likely to be complex in this region, which may partly explain the only modest correlation of our coral record with monthly rainfall, and the complete lack of a correlation at annual resolution. This result reinforces that while rainfall is a driver of CDOM flux and hence of coral luminescence, the relationship is likely to be controlled by complex hydrological processes in peatland regions.

These complexities of peatland hydrology would likely dampen the seasonal variability in fluvial CDOM flux relative to the seasonal variability in rainfall. Consistent with this expectation, ChunHock et al. (2020) inferred that quarterly average fluxes of tDOC from rivers in Sarawak as estimated by satellite remote sensing varied by at most threefold from 2013 to 2018. In contrast, our reconstructed CDOM record shows high seasonal variability, with very low CDOM values during the Southwest Monsoon, which suggests that it might also be driven by seasonal changes in processes removing CDOM. Experiments suggest that Southeast Asian peatland DOM is photolabile over short time-scales (Martin et al., 2018; Rixen et al., 2008). Photodegradation breaks down organic matter and can cause a rapid loss of CDOM (Helms et al., 2014; Miller & Zepp, 1995; Moran & Hodson, 1990; Stutter & Cains, 2016). The percentage cloud cover, number of cloudy days in our satellite CDOM record, and SST data are indicative of seasonal changes in irradiance, and therefore of the potential for CDOM photodegradation. While the lower rainfall during the less cloudy months of April to August will already reduce the CDOM flux to sea, the higher solar irradiance most likely reduces the CDOM concentrations further still. In contrast, during the Northeast Monsoon months, the increase in rainfall-driven CDOM flux is probably amplified by a lower rate of photodegradation. While CDOM mostly mixes conservatively across estuaries in Sarawak, the absorption and fluorescence spectral characteristics measured in coastal waters of Sarawak are consistent with a contribution from partly photodegraded tDOC, and further photodegradation was observed when seawater from this region was exposed to sunlight (Martin et al., 2018; Zhou et al., 2019). Along similar lines, pCO_2 data indicate that a large proportion of peat-derived tDOC is remineralized in coastal waters off Sumatra, suggesting that this material is biogeochemically labile after mixing across estuaries (Wit et al., 2018).

In addition to rainfall and photodegradation, seasonal variation in physical dilution by currents might impact coastal CDOM concentrations. However, our site most likely experiences stronger mixing and dilution during the stormier Northeast Monsoon period than during other seasons, as shown by the higher average wind speeds during December to February (Figure S1). Physical modeling further confirms that water residence times along the entire coastline of Sarawak (and across the entire Sunda Shelf) are lowest during the Northeast Monsoon (Mayer et al., 2015). Our data thus show that the CDOM concentration in coastal waters is highest at the time when the physical CDOM dilution rate is greatest but decreases to the lowest values as the dilution rate also decreases. Conversely, the potential for photodegradation of CDOM increases

during the less cloudy months from April to August, coincident with the observed seasonal decrease in CDOM. While our data thus confirm that coral luminescence can be used to reconstruct hydrological variability, it may also be important to consider potential variability in processes removing terrestrial CDOM over the time-scale of the record.

On interannual time-scales, the coral CDOM record shows notable changes in seasonal variability, especially with the period 1996–2001. Our data show that years that have high Northeast Monsoon rainfall (i.e., ≥700 mm/month) have high CDOM maxima but subsequently low CDOM minima. On the other hand, years (particularly consecutive years such as between 1996 to 2001) that do not have such a large peak rainfall during the Northeast Monsoon have lower CDOM maxima but also higher CDOM minima. This would be consistent with the fact that rainfall acts both as a driver of tDOC flux but also acts to dilute or concentrate tDOC. During 1996–2001, the Northeast Monsoon rainfall is some of the lowest observed, which would necessarily limit the total quantity of tDOC flux. However, rainfall amount in the other seasons, that is, other than the Northeast Monsoon, is similar to that in other years. Because of the lower annual rainfall during this 1996-2001 period, the riverine tDOC concentration is likely increased because of overall lower rainfall-driven dilution, which would then result in a larger tDOC flux during the Southwest Monsoon, and a corresponding increase in the CDOM minima during these years. Analysis of more coral-based CDOM reconstructions from tropical peatland-influenced regions will help to shed light on the drivers of such interannual variability and on the hydrological drivers of peatland tDOC fluxes.

The 24-year long Talang record did not show a statistically significant long-term trend in CDOM. Most of the forest within the Samunsam catchment is protected and has remained relatively intact, including the peatlands, as shown by the Centre for International Forestry Atlas (accessible under https://atlas.cifor.org, Gaveau et al., 2016). This indicates that forest and peatland protection measures can be effective at stabilizing soil carbon pools. Our study demonstrates that coral luminescence G/B measurements can be used to reconstruct terrestrial CDOM, which provides a way to study land–ocean carbon fluxes and promises to reduce the severe lack of historical biogeochemical data in tropical regions.

Data Availability Statement

All data for this study can be found under https://doi.org/10.21979/N9/5CZV22

Acknowledgments
The authors thank Gan Min Chong and students from UNIMAS and Swinburne Sarawak for assistance during coral coring. The coral core was collected under permit number NCCD.907.4.4(-JLD.12)-151 and park permit no. 89/2016. The authors would also like to thank the editor and two anonymous reviewers for their time and helpful suggestions. Nikita Kaushal would like to thank Dr. Ashok Kaushal for the first introduction to remote sensing. The authors thank Jennifer Chong from DHI Group for providing information about the current direction in the study region. This work was funded through a Singapore Ministry of Education Academic Research Fund Tier 1 grant to Patrick Martin (RG123/18), a National Research Foundation (NRF)–Royal Society Commonwealth Postdoctoral Fellowship to Nikita Kaushal (NRF-SCS-ICFC2017-01), and the Singapore NRF Fellowship scheme awarded to Nathalie F. Goodkin (NRFF-2012-03), administered by Earth Observatory of Singapore under the Research Centres of Excellence initiative. Nagur Cherukuru acknowledges Australian Academy of Sciences funding support through Regional Collaborations Programme for continued development of the remote sensing model. Moritz Müller acknowledges funding from the Sarawak Multimedia Authority under the Sarawak Digital Centre of Excellence. Aazani Mujahid acknowledges GRA and research funding under GL/F07/UMS/07/2017. Jen N. Lee acknowledges funding from Malaysia Fundamental Research Grant Scheme (FRGS/2/2013/STWN04/UMT/03/1). The authors declare no conflicts of interest.

References

Aksnes, D., Dupont, N., Staby, A., Fiksen, Ø., Kaartvedt, S., & Aure, J. (2009). Coastal water darkening and implications for mesopelagic regime shifts in Norwegian fjords. *Marine Ecology Progress Series*, *387*, 39–49. https://doi.org/10.3354/meps08120

Astoreca, R., Rousseau, V., & Lancelot, C. (2009). Colored dissolved organic matter (CDOM) in Southern North Sea waters: Optical characterization and possible origin. *Estuarine, Coastal and Shelf Science*, *85*(4), 633–640. https://doi.org/10.1016/j.ecss.2009.10.010

Bushaw, K. L., Zepp, R. G., Tarr, M. A., Schulz-Jander, D., Bourbonniere, R. A., Hodson, R. E., et al. (1996). Photochemical release of biologically available nitrogen from aquatic dissolved organic matter. *Nature*, *381*(6581), 404–407. https://doi.org/10.1038/381404a0

Butman, D. E., Wilson, H. F., Barnes, R. T., Xenopoulos, M. A., & Raymond, P. A. (2015). Increased mobilization of aged carbon to rivers by human disturbance. *Nature Geosciences*, *8*(2), 112–116. https://doi.org/10.1038/ngeo2322

Carr, N., Davis, C. E., Blackbird, S., Daniels, L. R., Preece, C., Woodward, M., & Mahaffey, C. (2019). Seasonal and spatial variability in the optical characteristics of DOM in a temperate shelf sea. *Progress in Oceanography*, *177*, 101929. https://doi.org/10.1016/j.pocean.2018.02.025

Cherukuru, N., Martin, P., Sanwlani, N., Mujahid, A., & Müller, M. (2021). A semi-analytical optical remote sensing model to estimate suspended sediment and dissolved organic carbon in tropical coastal waters influenced by peatland-draining river discharges off Sarawak, Borneo. *Remote Sensing*, *13*(1), 99. https://doi.org/10.3390/rs13010099

ChunHock, S., Cherukuru, N., Mujahid, A., Martin, P., Sanwlani, N., Warneke, T., et al. (2020). A new remote sensing method to estimate river to ocean DOC flux in peatland dominated Sarawak Coastal regions, Borneo. *Remote Sensing*, *12*(20), 3380. https://doi.org/10.3390/rs12203380

Ciais, P., Sabine, C., Bala, G., Bopp, L., Brovkin, V., Canadell, J., et al. (2014). Carbon and other biogeochemical cycles. In T. F. Stocker, D. Qin, G.-K. Plattner, M. Tignor, S. K. Allen, J. Boschung, et al. (Eds.), *Climate change 2013: The physical science basis. Contribution of Working Group I to the Fifth Assessment Report of the Intergovernmental Panel on Climate Change*. Cambridge University Press.

Clark, J. M., Lane, S. N., Chapman, P. J., & Adamson, J. K. (2007). Export of dissolved organic carbon from an upland peatland during storm events: Implications for flux estimates. *Journal of Hydrology*, *347*(3), 438–447. https://doi.org/10.1016/j.jhydrol.2007.09.030

Clark, J. M., Lane, S. N., Chapman, P. J., & Adamson, J. K. (2008). Link between DOC in near surface peat and stream water in an upland catchment. *The Science of the Total Environment*, *404*(2), 308–315. https://doi.org/10.1016/j.scitotenv.2007.11.002

Coble, P. G. (2007). Marine optical biogeochemistry: The chemistry of ocean color. *Chemistry Reviews*, *107*(2), 402–418. https://doi.org/10.1021/cr050350+

Cole, J. J., Prairie, Y. T., Caraco, N. F., McDowell, W. H., Tranvik, L. J., Striegl, R. G., et al. (2007). Plumbing the global carbon cycle: Integrating inland waters into the terrestrial carbon budget. *Ecosystems*, *10*(1), 172–185. https://doi.org/10.1007/s10021-006-9013-8

Dai, M., Yin, Z., Meng, F., Liu, Q., & Cai, W.-J. (2012). Spatial distribution of riverine DOC inputs to the ocean: An updated global synthesis. *Current Opinion in Environmental Sustainability*, *4*(2), 170–178. https://doi.org/10.1016/j.cosust.2012.03.003

Dommain, R., Couwenberg, J., Glaser, P. H., Joosten, H., & Suryadiputra, I. N. N. (2014). Carbon storage and release in Indonesian peatlands since the last deglaciation. *Quaternary Science Reviews*, *97*, 1–32. https://doi.org/10.1016/j.quascirev.2014.05.002

D'Sa, E. J., Miller, R. L., & Castillo, C. D. (2006). Bio-optical properties and ocean color algorithms for coastal waters influenced by the Mississippi River during a cold front. *Applied Optics*, *45*(28), 7410–7428. https://doi.org/10.1364/AO.45.007410

Dunne, R., & Brown, B. (1996). Penetration of solar UVB radiation in shallow tropical waters and its potential biological effects on coral reefs; results from the central Indian Ocean and Andaman Sea. *Marine Ecology Progress Series*, *144*, 109–118. https://doi.org/10.3354/meps144109

Evans, C. D., Monteith, D. T., & Cooper, D. M. (2005). Long-term increases in surface water dissolved organic carbon: Observations, possible causes and environmental impacts. *Environmental Pollution*, *137*(1), 55–71. https://doi.org/10.1016/j.envpol.2004.12.031

Fichot, C. G., & Benner, R. (2012). The spectral slope coefficient of chromophoric dissolved organic matter (S 275-295) as a tracer of terrigenous dissolved organic carbon in river-influenced ocean margins. *Limnology & Oceanography*, *57*(5), 1453–1466. https://doi.org/10.4319/lo.2012.57.5.1453

Fichot, C. G., Lohrenz, S. E., & Benner, R. (2014). Pulsed, cross-shelf export of terrigenous dissolved organic carbon to the Gulf of Mexico. *Journal of Geophysical Research and Oceans*, *119*(2), 1176–1194. https://doi.org/10.1002/2013JC009424

Frigstad, H., Andersen, T., Hessen, D. O., Jeansson, E., Skogen, M., Naustvoll, L.-J., et al. (2013). Long-term trends in carbon, nutrients and stoichiometry in Norwegian coastal waters: Evidence of a regime shift. *Progress in Oceanography*, *111*, 113–124. https://doi.org/10.1016/j.pocean.2013.01.006

Gandois, L., Cobb, A. R., Hei, I. C., Lim, L. B. L., Salim, K. A., & Harvey, C. F. (2013). Impact of deforestation on solid and dissolved organic matter characteristics of tropical peat forests: Implications for carbon release. *Biogeochemistry*, *114*(1), 183–199. https://doi.org/10.1007/s10533-012-9799-8

Gattuso, J.-P., Gentili, B., Duarte, C. M., Kleypas, J. A., Middelburg, J. J., & Antoine, D. (2006). Light availability in the coastal ocean: Impact on the distribution of benthic photosynthetic organisms and contribution to primary production. *Biogeosciences Discussions*, *3*(4), 895–959. https://doi.org/10.5194/bg-3-489-2006

Gaveau, D. L. A., Sheil, D., Husnayaen, M. A., Arjasakusuma, S., Ancrenaz, M., et al. (2016). Rapid conversions and avoided deforestation: Examining four decades of industrial plantation expansion in Borneo. *Scientific Reports*, *6*(1), 32017. https://doi.org/10.1038/srep32017

Grove, C. A., Nagtegaal, R., Zinke, J., Scheufen, T., Koster, B., Kasper, S., et al. (2010). River runoff reconstructions from novel spectral luminescence scanning of massive coral skeletons. *Coral Reefs*, *29*, 579–591. https://doi.org/10.1007/s00338-010-0629-y

Grove, C. A., Rodriguez-Ramirez, A., Merschel, G., Tjallingii, R., Zinke, J., Macia, A., & Brummer, G.-J. A. (2015). UV-Spectral Luminescence Scanning: Technical Updates and Calibration Developments. In I. W. Croudace, & R. G. Rothwell (Eds.), *Micro-XRF studies of sediment cores: Applications of a non-destructive tool for the environmental sciences* (pp. 563–581). Springer Netherlands. https://doi.org/10.1007/978-94-017-9849-5_23

Grove, C. A., Zinke, J., Peeters, F., Park, W., Scheufen, T., Kasper, S., et al. (2013). Madagascar corals reveal a multidecadal signature of rainfall and river runoff since 1708. *Climate of the Past*, *9*(2), 641–656. https://doi.org/10.5194/cp-9-641-2013

Grove, C. A., Zinke, J., Scheufen, T., Maina, J., Epping, E., Boer, W., et al. (2012). Spatial linkages between coral proxies of terrestrial runoff across a large embayment in Madagascar. *Biogeosciences*, *9*(8), 3063–3081. https://doi.org/10.5194/bg-9-3063-2012

Helms, J. R., Mao, J., Stubbins, A., Schmidt-Rohr, K., Spencer, R. G. M., Hernes, P. J., & Mopper, K. (2014). Loss of optical and molecular indicators of terrigenous dissolved organic matter during long-term photobleaching. *Aquatic Sciences*, *76*(3), 353–373. https://doi.org/10.1007/s00027-014-0340-0

Helms, J. R., Stubbins, A., Perdue, E. M., Green, N. W., Chen, H., & Mopper, K. (2013). Photochemical bleaching of oceanic dissolved organic matter and its effect on absorption spectral slope and fluorescence. *Marine Chemistry*, *155*, 81–91. https://doi.org/10.1016/j.marchem.2013.05.015

Isdale, P. J. (1984). Fluorescent bands in massive corals record centuries of coastal rainfall. *Nature*, *310*(5978), 578–579. https://doi.org/10.1038/310578a0

Isdale, P. J., Stewart, B. J., Tickle, K. S., & Lough, J. M. (1998). Palaeohydrological variation in a tropical river catchment: A reconstruction using fluorescent bands in corals of the Great Barrier Reef, Australia. *The Holocene*, *8*(1), 1–8. https://doi.org/10.1191/095968398670905088

Jones, P., & Harris, I. (2008). *Climatic Research Unit (CRU) time-series datasets of variations in climate with variations in other phenomena* (p. 15). NCAS British Atmospheric Data Centre.

Jones, R. I. (1998). Phytoplankton, primary production and nutrient cycling. *Aquatic Humic Substances*, 145–175. https://doi.org/10.1007/978-3-662-03736-2_8

Karlsson, K.-G., Anttila, K., Trentmann, J., Stengel, M., Meirink, J. F., Devasthale, A., et al. (2017). *CLARA-A2: CM SAF cLoud, Albedo and surface RAdiation dataset from AVHRR data—Edition 2* (p. 12.4 TiB, NetCDF v4). Satellite Application Facility on Climate Monitoring (CM SAF). https://doi.org/10.5676/EUM_SAF_CM/CLARA_AVHRR/V002

Kaushal, N., Yang, L., Tanzil, J. T. I., Lee, J. N., Goodkin, N. F., & Martin, P. (2020). Sub-annual fluorescence measurements of coral skeleton: Relationship between skeletal luminescence and terrestrial humic-like substances. *Coral Reefs*, *39*(5), 1257–1272. https://doi.org/10.1007/s00338-020-01959-x

Kowalczuk, P., Olszewski, J., Darecki, M., & Kaczmarek, S. (2005). Empirical relationships between colored dissolved organic matter (CDOM) absorption and apparent optical properties in Baltic Sea waters. *International Journal of Remote Sensing*, *26*(2), 345–370. https://doi.org/10.1080/01431160410001720270

Liu, B., D'Sa, E. J., & Joshi, I. (2019). Multi-decadal trends and influences on dissolved organic carbon distribution in the Barataria Basin, Louisiana from in-situ and Landsat/MODIS observations. *Remote Sensing of Environment*, *228*, 183–202. https://doi.org/10.1016/j.rse.2019.04.023

Lough, J. M. (2007). Tropical river flow and rainfall reconstructions from coral luminescence: Great Barrier Reef, Australia. *Paleoceanography*, *22*(2). https://doi.org/10.1029/2006PA001377

Lough, J. M., Barnes, D., & McAllister, F. (2002). Luminescent lines in corals from the Great Barrier Reef provide spatial and temporal records of reefs affected by land runoff. *Coral Reefs*, *21*(4), 333–343. https://doi.org/10.1007/s00338-002-0253-6

Maina, J., de Moel, H., Vermaat, J. E., Henrich Bruggemann, J., Guillaume, M. M. M., Grove, C. A., et al. (2012). Linking coral river runoff proxies with climate variability, hydrology and land-use in Madagascar catchments. *Marine Pollution Bulletin*, *64*(10), 2047–2059. https://doi.org/10.1016/j.marpolbul.2012.06.027

Mannino, A., Russ, M. E., & Hooker, S. B. (2008). Algorithm development and validation for satellite-derived distributions of DOC and CDOM in the U.S. Middle Atlantic Bight. *Journal of Geophysical Research: Oceans*, *113*(C7). https://doi.org/10.1029/2007JC004493

Martin, P., Cherukuru, N., Tan, A. S. Y., Sanwlani, N., Mujahid, A., & Müller, M. (2018). Distribution and cycling of terrigenous dissolved organic carbon in peatland-draining rivers and coastal waters of Sarawak, Borneo. *Biogeosciences*, *15*(22), 6847–6865. https://doi.org/10.5194/bg-15-6847-2018

Mascarenhas, V. J., Voß, D., Wollschlaeger, J., & Zielinski, O. (2017). Fjord light regime: Bio-optical variability, absorption budget, and hyperspectral light availability in Sognefjord and Trondheimsfjord, Norway. *Journal of Geophysical Research: Oceans*, *122*(5), 3828–3847. https://doi.org/10.1002/2016JC012610

Matthews, B. J. H., Jones, A. C., Theodorou, N. K., & Tudhope, A. W. (1996). Excitation-emission-matrix fluorescence spectroscopy applied to humic acid bands in coral reefs. *Marine Chemistry*, *55*(3), 317–332. https://doi.org/10.1016/S0304-4203(96)00039-4

Mayer, B., Stacke, T., Stottmeister, I., & Pohlmann, T. (2015). Sunda shelf seas: Flushing rates and residence times. *Ocean Science Discussions*, *12*(3), 863–895. https://doi.org/10.5194/osd-12-863-2015

Miller, W. L., & Zepp, R. G. (1995). Photochemical production of dissolved inorganic carbon from terrestrial organic matter: Significance to the oceanic organic carbon cycle. *Geophysical Research Letters*, *22*(4), 417–420. https://doi.org/10.1029/94GL03344

Monteith, D. T., Stoddard, J. L., Evans, C. D., de Wit, H. A., Forsius, M., Høgåsen, T., et al. (2007). Dissolved organic carbon trends resulting from changes in atmospheric deposition chemistry. *Nature*, *450*(7169), 537–540. https://doi.org/10.1038/nature06316

Moore, S., Evans, C. D., Page, S. E., Garnett, M. H., Jones, T. G., Freeman, C., et al. (2013). Deep instability of deforested tropical peatlands revealed by fluvial organic carbon fluxes. *Nature*, *493*(7434), 660–663. https://doi.org/10.1038/nature11818

Moore, T. R., & Jackson, R. J. (1989). Dynamics of dissolved organic carbon in forested and disturbed catchments, Westland, New Zealand: 2. Larry River. *Water Resources Research*, *25*(6), 1331–1339. https://doi.org/10.1029/WR025i006p01331

Moran, M. A., & Hodson, R. E. (1990). Bacterial production on humic and nonhumic components of dissolved organic carbon. *Limnology & Oceanography*, *35*(8), 1744–1756. https://doi.org/10.4319/lo.1990.35.8.1744

Nagtegaal, R., Grove, C. A., Kasper, S., Zinke, J., Boer, W., & Brummer, G.-J. A. (2012). Spectral luminescence and geochemistry of coral aragonite: Effects of whole-core treatment. *Chemical Geology*, *318–319*, 6–15. https://doi.org/10.1016/j.chemgeo.2012.05.006

Noacco, V., Wagener, T., Worrall, F., Burt, T. P., & Howden, N. J. K. (2017). Human impact on long-term organic carbon export to rivers. *Journal of Geophysical Research: Biogeosciences*, *122*(4), 947–965. https://doi.org/10.1002/2016JG003614

Odermatt, D., Gitelson, A., Brando, V. E., & Schaepman, M. (2012). Review of constituent retrieval in optically deep and complex waters from satellite imagery. *Remote Sensing of Environment*, *118*, 116–126. https://doi.org/10.1016/j.rse.2011.11.013

Osburn, C. L., Kinsey, J. D., Bianchi, T. S., & Shields, M. R. (2019). Formation of planktonic chromophoric dissolved organic matter in the ocean. *Marine Chemistry*, *209*, 1–13. https://doi.org/10.1016/j.marchem.2018.11.010

Paillard, D., Labeyrie, L., & Yiou, P. (1996). Macintosh Program performs time-series analysis. *Eos Transactions American Geophysical Union*, *77*(39), 379. https://doi.org/10.1029/96EO00259

Painter, S. C., Lapworth, D. J., Woodward, E. M. S., Kroeger, S., Evans, C. D., Mayor, D. J., & Sanders, R. J. (2018). Terrestrial dissolved organic matter distribution in the North Sea. *The Science of the Total Environment*, *630*, 630–647. https://doi.org/10.1016/j.scitotenv.2018.02.237

Piccolo, A., Spaccini, R., Drosos, M., Vinci, G., & Cozzolino, V. (2018). Chapter 4—The molecular composition of humus carbon: Recalcitrance and reactivity in soils. In C. Garcia, P. Nannipieri, & T. Hernandez (Eds.), *The future of soil carbon* (pp. 87–124). Academic Press. https://doi.org/10.1016/B978-0-12-811687-6.00004-3

Pienitz, R., & Vincent, W. F. (2000). Effect of climate change relative to ozone depletion on UV exposure in subarctic lakes. *Nature*, *404*(6777), 484–487. https://doi.org/10.1038/35006616

Rayner, N. A., Parker, D. E., Horton, E. B., Folland, C. K., Alexander, L. V., Rowell, D. P., et al. (2003). Global analyses of sea surface temperature, sea ice, and night marine air temperature since the late nineteenth century. *Journal of Geophysical Research*, *108*(D14). https://doi.org/10.1029/2002JD002670

Rixen, T., Baum, A., Pohlmann, T., Balzer, W., Samiaji, J., & Jose, C. (2008). The Siak, a tropical black water river in central Sumatra on the verge of anoxia. *Biogeochemistry*, *90*(2), 129–140. https://doi.org/10.1007/s10533-008-9239-y

Rixen, T., Baum, A., Wit, F., & Samiaji, J. (2016). Carbon leaching from tropical peat soils and consequences for carbon balances. *Frontiers in Earth Science*, *4*. https://doi.org/10.3389/feart.2016.00074

Rodriguez-Ramirez, A., Grove, C. A., Zinke, J., Pandolfi, J. M., & Zhao, J. (2014). Coral luminescence identifies the Pacific decadal oscillation as a primary driver of river runoff variability impacting the Southern Great Barrier Reef. *PLoS One*, *9*(1), e84305. https://doi.org/10.1371/journal.pone.0084305

Semiletov, I., Pipko, I., Gustafsson, Ö., Anderson, L. G., Sergienko, V., Pugach, S., et al. (2016). Acidification of East Siberian Arctic Shelf waters through addition of freshwater and terrestrial carbon. *Nature Geosciences*, *9*(5), 361–365. https://doi.org/10.1038/ngeo2695

Shanmugam, P. (2011). New models for retrieving and partitioning the colored dissolved organic matter in the global ocean: Implications for remote sensing. *Remote Sensing of Environment*, *115*(6), 1501–1521. https://doi.org/10.1016/j.rse.2011.02.009

Siswanto, E., Tang, J., Yamaguchi, H., Ahn, Y.-H., Ishizaka, J., Yoo, S., et al. (2011). Empirical ocean-color algorithms to retrieve chlorophyll-a, total suspended matter, and colored dissolved organic matter absorption coefficient in the Yellow and East China Seas. *Journal of Oceanography*, *67*(5), 627–650. https://doi.org/10.1007/s10872-011-0062-z

Stedmon, C. A., & Markager, S. (2001). The optics of chromophoric dissolved organic matter (CDOM) in the Greenland Sea: An algorithm for differentiation between marine and terrestrially derived organic matter. *Limnology & Oceanography*, *46*(8), 2087–2093. https://doi.org/10.4319/lo.2001.46.8.2087

Stutter, M. I., & Cains, J. (2016). The mineralisation of dissolved organic matter recovered from temperate waterbodies during summer. *Aquatic Sciences*, *78*(3), 447–462. https://doi.org/10.1007/s00027-015-0446-z

Susic, M., Boto, K., & Isdale, P. (1991). Fluorescent humic acid bands in coral skeletons originate from terrestrial runoff. *Marine Chemistry*, *33*(1), 91–104. https://doi.org/10.1016/0304-4203(91)90059-6

Tambutté, E., Tambutté, S., Segonds, N., Zoccola, D., Venn, A., Erez, J., & Allemand, D. (2012). Calcein labelling and electrophysiology: Insights on coral tissue permeability and calcification. *Proceedings of the Royal Society B*, *279*(1726), 19–27. https://doi.org/10.1098/rspb.2011.0733

Tanzil, J. T. I., Goodkin, N. F., Sin, T. M., Chen, M. L., Fabbro, G. N., Boyle, E. A., et al. (2019). Multi-colony coral skeletal Ba/Ca from Singapore's turbid urban reefs: Relationship with contemporaneous in-situ seawater parameters. *Geochimica et Cosmochimica Acta*, *250*, 191–208. https://doi.org/10.1016/j.gca.2019.01.034

Tanzil, J. T. I., Lee, J. N., Brown, B. E., Quax, R., Kaandorp, J. A., Lough, J. M., & Todd, P. A. (2016). Luminescence and density banding patterns in massive Porites corals around the Thai-Malay Peninsula, Southeast Asia. *Limnology & Oceanography*, *61*(6), 2003–2026. https://doi.org/10.1002/lno.10350

Tudhope, A. W., Lea, D. W., Shimmield, G. B., Chilcott, C. P., & Head, S. (1996). Monsoon climate and Arabian sea coastal upwelling recorded in massive corals from Southern Oman. *PALAIOS*, *11*(4), 347–361. https://doi.org/10.2307/3515245

Ward, N. D., Bianchi, T. S., Medeiros, P. M., Seidel, M., Richey, J. E., Keil, R. G., & Sawakuchi, H. O. (2017). Where carbon goes when water flows: Carbon cycling across the aquatic continuum. *Frontiers in Marine Science*, *4*. https://doi.org/10.3389/fmars.2017.00007

Wauthy, M., Rautio, M., Christoffersen, K. S., Forsström, L., Laurion, I., Mariash, H. L., et al. (2018). Increasing dominance of terrigenous organic matter in circumpolar freshwaters due to permafrost thaw. *Limnology & Oceanography*, *3*(3), 186–198. https://doi.org/10.1002/lol2.10063

Werdell, P. J., Franz, B. A., Bailey, S. W., Feldman, G. C., Boss, E., Brando, V. E., et al. (2013). Generalized ocean color inversion model for retrieving marine inherent optical properties. *Applied Optics*, *52*(10), 2019–2037. https://doi.org/10.1364/AO.52.000027

Wit, F., Rixen, T., Baum, A., Pranowo, W. S., & Hutahaean, A. A. (2018). The Invisible Carbon Footprint as a hidden impact of peatland degradation inducing marine carbonate dissolution in Sumatra, Indonesia. *Scientific Reports*, *8*(1), 1–10. https://doi.org/10.1038/s41598-018-35769-7

Yupi, H. M., Inoue, T., & Bathgate, J. (2016). Concentrations, loads and yields of organic carbon from two tropical peat swamp forest streams in Riau Province, Sumatra, Indonesia. *Mires & Peat*, *18*, 1–15. https://doi.org/10.19189/MaP.2015.OMB.181

Zhou, Y., Martin, P., & Müller, M. (2019). Composition and cycling of dissolved organic matter from tropical peatlands of coastal Sarawak, Borneo, revealed by fluorescence spectroscopy and parallel factor analysis. *Biogeosciences*, *16*(13), 2733–2749. https://doi.org/10.5194/bg-16-2733-2019